ECS Electrochemistry Letters, **2** (4) A33-A35 (2013)
2162-8726/2013/2(4)/A33/3/$31.00 © The Electrochemical Society

Modeling and Experimental Study of Porous Carbon Cathodes in Li-O_2 Cells with Non-Aqueous Electrolyte

Vitaliy Y. Nimon,[a,*,z] Steven J. Visco,[a,*] Lutgard C. De Jonghe,[a] Yury M. Volfkovich,[b] and Daniil A. Bograchev[b]

[a] *PolyPlus Battery Company, Berkeley, California 94710, USA*
[b] *Frumkin Institute of Physical Chemistry and Electrochemistry RAS, Moscow, Russia*

We performed mathematical modeling and experimental study of porous carbon air cathodes in Li-O_2 cells having a non-aqueous electrolyte based on dimethylformamide (DMF). Using the method of standard contact porosimetry, we characterized the porous structure of undischarged, partially discharged, and fully discharged Ketjenblack carbon black-based air cathodes and determined that deposition of solid discharge product occurs within small mesopores with radii of up to 10 nm. We propose a novel mathematical model of air cathode, which takes into account its porous structure and accurately describes the discharge behavior of Li-O_2 cells with the DMF-based electrolyte.
 [DOI: 10.1149/2.004304eel]

Manuscript submitted September 28, 2012; revised manuscript received December 28, 2012. Published January 28, 2013.

Lithium-Air batteries have attracted a lot of attention since they have the potential to achieve significantly higher values of specific energy than Li-Ion batteries.[1–3] Invention of a protected lithium electrode (PLE) by PolyPlus Battery Company[1,4,5] enabled development of Li-Air batteries with aqueous and aggressive non-aqueous electrolytes that are not directly stable to lithium metal, and therefore, could not be used in Li-Air batteries without lithium protection. This is particularly important since conventional aprotic solvents used in Li-Ion and Li metal batteries, such as organic carbonates and ethers, react with products of oxygen reduction and, therefore, cannot be used in Li-Air batteries.[3] In this paper we present the study of cathode processes in Li-O_2 cells with a non-aqueous electrolyte based on dimethylformamide (DMF), which itself is highly reactive toward lithium and can be used only in combination with the PLE.[6] Oxygen reduction processes have been extensively studied in solutions containing DMF and tetraalkylammonium salts[7–9] and DMF is expected to be kinetically stable against the products of oxygen reduction. Despite the possibility that carbon can be oxidized during cell charge, it is presently the cathode material of choice in Li-Air batteries under development[2,3] and was used in our discharge and porosimetry experiments described below.

There have been few theoretical articles describing the processes taking place in Li-O_2 cells. In[10] these processes were described using a single cathode pore model. In model[11] it was assumed that solid discharge products were deposited as a uniformly growing dense film on the surface of a smooth glassy carbon electrode or on the surface of spherical carbon particles of a porous air cathode. It was concluded that porous cathodes behaved similarly to smooth electrodes in regard to precipitate formation. However, model[11] did not take into consideration the realities of air cathode pore size distribution and therefore cannot be used for optimization of the cathode porous structure.

The present study includes the following: experimental measurements of pore size distribution in the air cathode before discharge and at various stages of discharge, the development of an improved model of air cathode behavior taking into account its porous structure, and comparison of calculated discharge curves with experimental ones.

Model Development

We assume that the solid discharge product fills the entire volume of a pore rather than covers its walls with a surface film. For micropores this is consistent with the experimentally verified theory of volumetric filling.[12,13] For macropores our model is consistent with the experimental studies of a carbon cathode in Li - thionyl chloride batteries,[14] which showed that at the beginning of discharge the solid discharge product (LiCl) filled the largest pores first and then as the discharge progressed it continued filling progressively smaller pores. The experimental data presented below also strongly indicate volumetric filling of pores.

Data presented in[14] in combination with our own experimental data suggest that the order of pore filling – from largest to smallest or vice versa – depends on the sign (positive or negative) of the difference between two interface energies: that of the liquid electrolyte / pore wall interface and that of the discharge product / pore wall interface. According to our experimental data described below, in the Li-O_2 system having a DMF-based electrolyte and Li_2O_2 as a solid discharge product, the volume fraction of the smallest cathode pores decreases as the discharge progresses. This can be explained by a strong adhesion of the solid discharge product (Li_2O_2) to the surface of the carbon electrode as described by the Kelvin equation.

Our model describes the transport of molecular oxygen and Li cations in liquid electrolyte as well as solid discharge product deposition within the porous structures of cathode and separator. The model also takes into consideration the diffusion of reaction products, their deposition governed by the Kelvin equation, changes in porosity as the solid discharge products precipitate, and the influence of these porosity changes on transport processes.

The overall reaction that takes place in a Li-O_2 cell during discharge is:

$$Li^+ + {}^1/_2O_2 + e^- \leftrightarrow {}^1/_2Li_2O_2$$

The modeled region spans the space between the left edge of the cathode compartment, which is in direct contact with the protected anode, and the right edge of the cathode compartment, where molecular oxygen enters the cathode. The origin of the x coordinate is located at the left edge of the separator. L_S is the separator thickness, L_C is the cathode thickness, $L = L_S + L_C$ is the total thickness of the modeled region. The schematic drawing of the Li-O_2 cell is presented in the online supplementary materials. It is assumed that the electrode is fully flooded.

The mass-transport equations for the battery's porous layers can be written as follows:

$$\frac{\partial \varepsilon c_{Li}}{\partial t} = \frac{\partial}{\partial x}\left(D^{eff}_{M,Li}\frac{\partial c_{Li}}{\partial x}\right) - \frac{1-t^0_+}{F}j^r, \quad [1]$$

$$\frac{\partial \varepsilon c_{O_2}}{\partial t} = \frac{\partial}{\partial x}\left(D^{eff}_{M,O_2}\frac{\partial c_{O_2}}{\partial x}\right) - \frac{j^r}{2F}, \quad [2]$$

$$\frac{\partial \varepsilon c_{Li_2O_2}}{\partial t} = \frac{\partial}{\partial x}\left(D^{eff}_{M,Li_2O_2}\frac{\partial c_{Li_2O_2}}{\partial x}\right) + \frac{j^r}{2F} - J_{dep}. \quad [3]$$

Equations 1–3 are the effective diffusion equations for Li cations with concentration c_{Li}, dissolved molecular oxygen with concentration c_{O_2}, and the reaction product with concentration $c_{Li_2O_2}$, which take into

*Electrochemical Society Active Member.
zE-mail: vnimon@polyplus.com

account the volumetric reaction current j^r and volumetric rate of precipitate formation J_{dep}. Here, ε and $D^{eff}_{M,s}$ are the porosity of the medium M and the effective diffusion coefficient of species s in the porous medium M, respectively, t^0_+ is the transference number for Li cations, F is Faraday's constant.

The effective diffusion coefficient of species s in the porous medium M is defined by the Bruggeman equation through diffusion in a free solution: $D^{eff}_{M,s} = D_s\varepsilon^{\alpha_M}$, where α_M is the Archie exponent of the medium M.

The volumetric reaction current j^r is zero at the separator and is defined by the specific surface density S and Butler-Volmer kinetics at the porous electrode:

$$j^r = Si_0\left(\frac{c_{O_2}}{c_{0,O_2}}\exp\left(\frac{\alpha\eta F}{RT}\right) - \exp\left(-\frac{(1-\alpha)\eta F}{RT}\right)\right), \quad [4]$$

where i_0 and α are the exchange current density and the transfer coefficient, respectively, c_{0,O_2} is the solubility limit of oxygen in electrolyte, $\eta = \varphi_e - \varphi_c$ is the overpotential of the reaction equal to the difference of electrolyte potential φ_e and cathode potential φ_c. Specific surface density S and porosity ε are functions of the coordinate along the thickness of the modeled region as well as of time:

$$\frac{\partial\varepsilon}{\partial t} = -\frac{\mu_{Li_2O_2}}{\rho_{Li_2O_2}}J_{dep}, \quad [5]$$

where $\mu_{Li_2O_2}$ is the molar mass and $\rho_{Li_2O_2}$ is the density of the solid discharge product.

The equation describing the rate of precipitation can be written as follows:

$$J_{dep} = K_M H(c_{Li_2O_2} - c_{Lim,Li_2O_2}) * \left(\frac{c_{Li_2O_2}}{c_{0,Lim,Li_2O_2}} - \frac{c_{Lim,Li_2O_2}}{c_{0,Lim,Li_2O_2}}\right)^2, \quad [6]$$

where $H(c_{Li_2O_2} - c_{Lim,Li_2O_2})$ is the Heaviside step function and K_M is the kinetic coefficient of precipitation, which depends on the properties of the porous medium M. Here, c_{0,Lim,Li_2O_2} is the solubility limit of Li_2O_2 in free electrolyte, c_{Lim,Li_2O_2} is the solubility limit of Li_2O_2 taking into consideration the Kelvin equation:

$$\ln\left(\frac{c_{Lim,Li_2O_2}}{c_{0,Lim,Li_2O_2}}\right) = \frac{2\gamma_M V_{Li_2O_2}}{r_{\min}RT}. \quad [7]$$

In the above equation, $\gamma_M = \gamma_{E,W} - \gamma_{Li_2O_2,W}, \gamma_{E,W}$ is the energy of the liquid electrolyte / pore wall interface and $\gamma_{Li_2O_2,W}$ is the energy of the discharge product / pore wall interface. Also in equation 7, $V_{Li_2O_2}$ is the molar volume of the reaction product, and $r_{\min}$ is the radius of the smallest pores filled with electrolyte; all pores with radii smaller than $r_{\min}$ are filled with the solid discharge product. For $\gamma_M < 0$, the energy of the discharge product / pore wall interface is greater than that of the liquid electrolyte / pore wall interface, and thus the precipitation of discharge product occurs in the small pores, which contribute most of the electrode surface area. As we describe below, this scenario is supported by our experimental results.

The charge transport equation in the electrolyte is:

$$\frac{\partial}{\partial x}\left(k^{eff}_M\frac{\partial\varphi_e}{\partial x}\right) + j^r(x) = 0. \quad [8]$$

As above, the properties of the porous structure are described by the model through the use of the Bruggeman equation for effective conductivity of electrolyte in the porous medium M: $k^{eff}_M = k\varepsilon^{\alpha_M}$, where the conductivity of the free solution k generally depends on concentration in a complex way.

The initial and boundary conditions as well as a table listing all model parameters and their values are presented in the online supplementary materials.

Experimental

In order to characterize the porosity of the air cathode we used the method of standard contact porosimetry (MSCP) described in[15,16] which is based on the principle of capillary equilibrium. The studied air cathode sample having an unknown pore size distribution and partially saturated with a working liquid (in our case, octane) was placed in capillary contact with a standard sample having a known pore size distribution, and the two bodies were allowed to reach capillary equilibrium. This process was repeated over a range of saturation values by allowing the working liquid to evaporate, and the capillary pressure curve of the studied sample was determined.

The details of porosimetry protocol as well as electrochemical cell design are described in the online supplementary materials. Experimental Li-O_2 cells were built with a PLE, a porous air cathode and a zirconia ZYF-50 separator. The air cathode was prepared from an active mass containing Ketjenblack carbon black and PTFE dispersion. The air cathode and the separator were completely filled with the non-aqueous electrolyte containing 0.5 M of $LiN(CF_3SO_2)_2$ salt dissolved in DMF. The cells were assembled and disassembled in the atmosphere of dry argon and discharged in the atmosphere of dry oxygen.

Results and Discussion

The obtained integral porograms for air cathodes before discharge, after partial discharge, and after full discharge are presented in Figure 1. The integral porogram for undischarged cathode indicates the presence of pores over a wide range of radii: from micropores with radii less than 1nm to macropores with radii as large as 10 μm (curve 1). After partial electrode discharge of 48% at a current density of 0.25 mA/cm^2 the volume of pores having radii in the range of 4 nm – 10 nm decreases indicating filling of the small mesopores with the solid discharge product (curve 2). Full discharge at the same current density leads to further filling of the pores in the same range of radii with the discharge product while the larger pores of the air cathode remain unfilled (curve 3). The observed reduction in overall volume fraction of mesopores with radii in the 4 nm – 10 nm range in the absence of a change in individual pore sizes as indicated by integral porograms in Figure 1 and by the lack of peak shift in the corresponding differential porograms unequivocally supports the model of volumetric pore filling. Furthermore, the porograms are inconsistent with the formation of a discharge product surface layer and consequent cathode passivation, which would have resulted in a uniform decrease of individual pore sizes.

In Figure 2 we compare the experimental (curves 1 and 4) and calculated (curves 2 and 3) discharge curves at two different discharge current densities. As seen, the proposed model yields discharge curves that fit the experimental discharge data quite well. The parameters used for calculation of discharge curves are listed in the table presented in the online supplementary materials. The values of the exchange current density (5*10^{-11} A/cm^2) and Archie's exponents for cathode and separator (3.7 and 1.5, respectively) were determined by curve fitting.

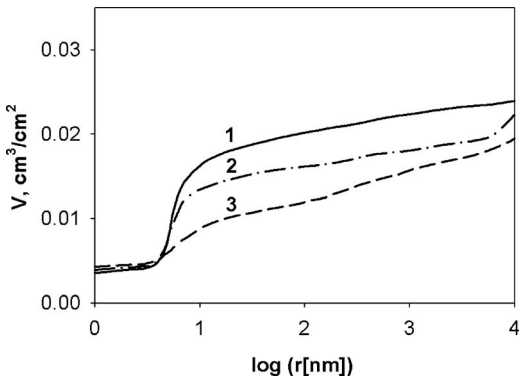

Figure 1. Integral porograms for air cathodes before discharge (curve 1), after partial discharge of 48% at 0.25 mA/cm^2 (curve 2), and after full discharge at 0.25 mA/cm^2 (curve 3).

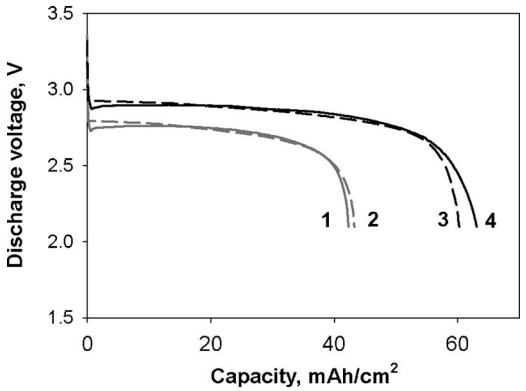

Figure 2. Comparison of experimental (solid lines, curves 1 and 4) and calculated (dashed lines, curves 2 and 3) discharge curves at two current densities (curves 1 and 2 at 0.25 mA/cm^2, curves 3 and 4 at 0.1 mA/cm^2).

Discharge capacities delivered at both current densities correlate well with amounts of solid discharge product calculated using the volume of the filled pores and theoretical density of Li_2O_2. Good agreement between the discharge curves derived from the model of volumetric pore filling and the experimental discharge curves lends further support to this model.

Conclusion

MSCP is a powerful technique for characterization of porous cathodes employed in Li-Air cells. Using MSCP, we obtained the first porosimetry results for partially and fully discharged air cathodes in Li-O_2 cells having an electrolyte stable toward products of oxygen reduction and therefore yielding a discharge product that consists primarily of Li_2O_2 rather than of electrolyte degradation products.

Based on the described model, the experimental results can be explained in the following manner. For a non-aqueous Li-O_2 cell having a DMF-based electrolyte and a porous air cathode based on Ketjenblack EC-600 JD carbon black, the delivered discharge capacity of the cathode is limited by the volume of solid discharge product that can be accommodated within the volume of small mesopores with radii of up to 10 nm until the liquid electrolyte volume fraction falls below the percolation threshold. We expect our model to be predictive for non-aqueous Li-O_2 cells over a broad range of solubility values of discharge product in the electrolyte. Also, this model elucidates the effect of the relative magnitudes of the liquid electrolyte / pore wall interface energy and the discharge product / pore wall interface energy on the delivered discharge capacity of non-aqueous Li-O_2 cells.

Acknowledgments

This work was funded in part by the ARPA-E of U. S. DOE, under Award Number DE-AR0000061.

References

1. S. J. Visco, E. Nimon, and L. C. De Jonghe, in *Encyclopedia of Electrochemical Power Sources Vol. 4*, J. Garche, Editor, p. 376, Elsevier, Amsterdam (2009).
2. J. Christiansen, P. Albertus, R. S. Sanchez-Carrera, T. Lohman, B. Kozinsky, R. Leitke, J. Ahmed, and A. Kojic, *J. Electrochem. Soc.*, **159**, R1 (2012).
3. P. G. Bruce, S. A. Freunberger, L. J. Hardwick, and J.-M. Tarascon, *Nature Materials*, **11**, 19 (2012).
4. S. J. Visco, B. D. Katz, Y. S. Nimon, and L. C. De Jonghe, U.S. Patent 7,282,295 (2007).
5. S. J. Visco and Y. S. Nimon, U.S. Patent 7,645,543 (2010).
6. S. J. Visco and Y. S. Nimon, U.S. Patent Application 2007/0117007 (2007).
7. D. L. Maricle and W. G. Hobson, *Analytical Chem.*, **37**, 1562 (1965).
8. M. E. Peover and B. S. White, *Electrochim. Acta*, **11**, 1061 (1966).
9. P. S. Jain and S. Lal, *Electrochim. Acta*, **27**, 759 (1982).
10. P. Andrei, J. P. Zheng, M. Hendrickson, and E. J. Plichta, *J. Electrochem. Soc.*, **157**, A1287 (2010).
11. P. Albertus, G. Girishkumar, B. McCloskey, R. S. Sanchez-Carrera, B. Kozinsky, J. Christensen, and A. C. Luntz, *J. Electrochem. Soc.*, **158**, A343 (2011).
12. M. M. Dubinin and G. M. Plavnik, *Carbon*, **6**, 183 (1968).
13. S. J. Gregg and K. S. W. Sing, *Adsorption, Surface Area and Porosity*, 2nd edition, Academic Press, New York (1982).
14. V. S. Bagotzky, Yu. M. Volfkovich, L. S. Kanevsky, A. M. Skundin, M. Broussely, P. Chenebault, and T. Caillaud, *Power Sources* 15, Ed. A. Attewel and T. Keily, Crowborough: Int. Power Sources Symp. Comm., 359 (1995).
15. Yu. M. Volfkovich and V. S. Bagotzky, *J. Power Sources*, **48**, 327 (1994).
16. Yu. M. Volfkovich, V. S. Bagotzky, V. E. Sosenkin, and I. A. Blinov, *Colloid Surf. A: Physocochem. Eng. Aspects*, **187/188**, 349 (2001).